
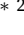


# Adding strain rate information into a short-term seismicity model improves forecasting performances: the case of Campi Flegrei, Italy

Giuseppe Petrillo <sup>1</sup>, Matteo Taroni <sup>\*</sup> <sup>2</sup>

<sup>1</sup>Earth Observatory of Singapore, Nanyang Technological University, Singapore, <sup>2</sup>Istituto Nazionale di Geofisica e Vulcanologia, Rome, Italy

**Author contributions:** *Conceptualization:* GP, MT. *Formal Analysis:* GP. *Writing - Original draft:* GP. *Writing - Review & Editing:* GP, MT. *Data Preparation:* MT. *Visualization:* GP, MT.

**Abstract** Campi Flegrei is a large active volcanic caldera in southern Italy, currently undergoing a prolonged phase of unrest that began in 2005, characterized by ground uplift and an increase in seismicity. Classical short-term seismicity models, such as the temporal Epidemic Type Aftershock Sequence (ETAS) model, rely exclusively on earthquake catalog data and do not incorporate external forcing mechanisms like crustal deformation. In this study, we extend the ETAS model by integrating strain rate information derived from GNSS measurements, allowing the background rate to vary in time through a data-driven convolution with an empirically estimated response kernel. Using eleven years of observations (2013–2024), we compare the forecasting performance of the classical and deformation-driven ETAS models. Our results show that including strain rate significantly improves forecasting ability, as evidenced by a lower Akaike Information Criterion (AIC). This finding suggests that incorporating geodetic signals into seismicity models enhances their physical realism and predictive skill, providing a promising path toward Operational Earthquake Forecasting in active volcanic regions.

Production Editor:  
Kiran Kumar Thingbaijam  
Handling Editor:  
Ryo Okuwaki  
Copy & Layout Editor:  
Théa Ragon

Received:  
August 1, 2025  
Accepted:  
September 9, 2025  
Published:  
September 17, 2025

## 1 Introduction

Forecasting seismicity at short time scales is a crucial yet challenging task, particularly in volcanic environments where the crustal stress field is modulated by transient and often poorly understood processes. Unlike tectonic regions, where long-term stressing is relatively uniform, volcanoes may exhibit rapid, localized, and nonlinear changes in stress due to magma migration, fluid injection, thermal expansion, and other aseismic processes (Chouet, 1996; Toda et al., 2002; Hainzl, 2003; Tramelli et al., 2021; Glazner and McNutt, 2021; Convertito et al., 2025). These processes generate strain that can, in turn, modulate seismic activity.

In recent years, the Campi Flegrei caldera in southern Italy has emerged as a key case for investigating such coupling. The area has been undergoing a long-term episode of uplift and seismic unrest since 2005, part of a broader bradyseismic cycle (Bevilacqua et al., 2024; De Martino et al., 2021; Godano et al., 2025). A notable feature of this unrest is the increase in both deformation and seismicity rates in Campi Flegrei during the last decade, with several events felt by the local population since 2020 (Iervolino et al., 2024). Despite its importance, the physical mechanisms linking deformation and seismicity remain unclear, and forecasting remains largely empirical.

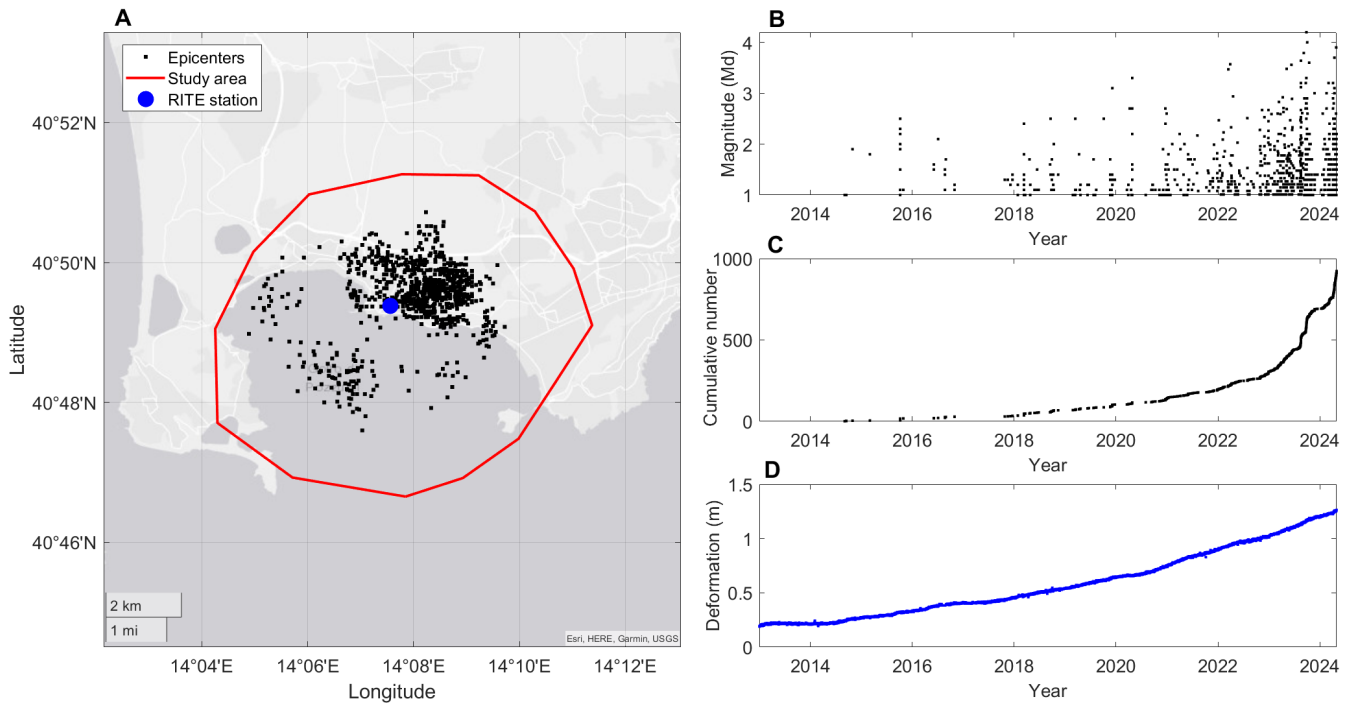
Most short-term forecasting models, such as the Epidemic Type Aftershock Sequence (ETAS) model (Ogata,

1988, 1998; Console et al., 2003; Petrillo and Lippiello, 2021, 2023; Petrillo and Zhuang, 2024), are based solely on seismicity catalogs. These models treat the seismic background rate  $\mu$  as stationary, or at best as a step-wise function to account for nonstationarities (Hainzl and Ogata, 2005). Some extensions, such as the nonstationary ETAS models proposed by Kumazawa and Ogata (2013, 2014) and successfully applied in tectonic region (Petrillo et al., 2024), allow the background rate to vary continuously in time by introducing time-varying parameters or spline functions. However, these models often suffer from possible overfitting and lack physical interpretability: the inferred variations in  $\mu(t)$  may fit the data well but offer limited insight into the underlying geophysical processes driving the changes in seismicity rate.

While ETAS has proven successful in tectonic settings, its ability to capture externally modulated seismicity, such as that observed at Campi Flegrei, is limited. In volcanic or geothermal systems, where deformation and fluid migration can transiently alter the stress field, there is a growing interest in extending ETAS-like models by incorporating geophysical or geodetic information to better account for the nonstationary nature of the background seismicity.

Some recent works have proposed the inclusion of fluid injection rates or stress perturbations as external forcings in seismicity models (Shcherbakov, 2024; Kim and Avouac, 2023). However, there remains a gap in applying these ideas to natural volcanic systems where

<sup>\*</sup>Corresponding author: matteo.taroni@ingv.it



**Figure 1** Seismicity and deformation data at Campi Flegrei caldera (2013–2024). (A) Map of the study area (red polygon) showing the epicenters of earthquakes (black dots) and the GNSS RITE station used in this study (blue circle). (B) Time series of earthquake magnitudes ( $M_d \geq 1$ ) within the study area. (C) Cumulative number of events over the same period, highlighting the acceleration of seismicity after 2020. (D) Vertical ground deformation (in meters) recorded at the RITE GNSS station, expressed as cumulative uplift, showing a continuous increase.

strain rate, measured via Global Positioning System (GPS) or Interferometric Synthetic Aperture Radar (InSAR), may act as a proxy for stress buildup and release.

In this work, we propose a deformation-driven ETAS model for the Campi Flegrei caldera. Our approach allows the background rate  $\mu(t)$  to vary in time as a convolution of the observed strain rate with an empirically estimated response kernel. This formulation aims to capture the delayed and distributed effect of deformation on seismicity, consistent with the viscoelastic behavior of volcanic crust. Using 11 years of seismic and GNSS data, we demonstrate that incorporating strain rate information leads to improved forecasting performance, as quantified by the Akaike Information Criterion (AIC) (Akaike, 1973).

Our study highlights how coupling seismicity models with geodetic observations can provide a more physically grounded framework for earthquake forecasting in volcanic environments, and it lays the groundwork for potential applications in Operational Earthquake Forecasting systems, i.e., the use of probabilistic models to provide time-dependent earthquake occurrence probabilities for decision making and risk mitigation (Mizrahi et al., 2024). It is important to emphasize that this study represents a preliminary proof-of-concept, focused on the Campi Flegrei case study. Further validation on independent datasets and in different volcanic or tectonic settings will be required before the proposed approach can be generalized or operationalized.

## 2 Data

In this work, we use two different datasets: a seismic catalog and a GNSS daily deformation dataset, both starting from 2013-01-01 to 2024-04-30. The complete part of the seismic catalog includes 925 events from magnitude  $M_d = 1.0$  inside the caldera and with a maximum depth of 4 km, since the large majority of the seismicity is concentrated in this area (see Fig. 1). The  $M_d$  magnitude, or duration magnitude, is a scale used to measure the size of smaller, local earthquakes; it is the standard in the Campi Flegrei seismic catalog (Bevilacqua et al., 2024). The magnitude of completeness of 1.0 is computed using the exponentiality test approach (Liliefors test, Herrmann and Marzocchi (2021)). Then, a check for a possible short-term incompleteness is performed using the Zhuang et al. (2017) method. For the deformation data, we use the GNSS RITE station (De Martino et al., 2021), located in the center of the caldera, similarly to other studies (Bevilacqua et al., 2024; Giudicepietro et al., 2025). To account for the temporal variability of the deformation (Bevilacqua et al., 2024), we computed a monthly averaged strain rate, using the same occurrence time of the events in our catalog (see Fig. 1).

## 3 The Deformation ETAS Model

The ETAS model (Ogata, 1985, 1988, 1998; Console et al., 2003) is a point process model widely used in statistical seismology to describe the clustered nature of earthquake occurrences. In its classical formulation, the

conditional intensity function  $\lambda(t)$ , which describes the expected rate of earthquakes at time  $t$  given the past history  $\mathcal{H}_t$ , is defined as:

$$\lambda(t|\mathcal{H}_t) = \mu + \sum_{t_i < t} K e^{\alpha(m_i - M_0)} (t - t_i + c)^{-p}, \quad (1)$$

where:  $\mu$  is the background rate of spontaneous events,  $K$  controls the productivity of aftershocks,  $\alpha$  quantifies the increase in triggering ability with magnitude,  $M_0$  is the lower magnitude threshold for triggering,  $c$  is the onset of the Omori Law,  $p$  governs the temporal decay of aftershock productivity, following Omori's law and  $\mathcal{H}_t$  is the past history.

Equation (1) represents a self-exciting process: each earthquake can generate its own aftershock sequence, which in turn can trigger additional events, thus forming a branching process. The model captures two main features of seismicity: (i) a stationary background rate due to tectonic loading, and (ii) clustering in time due to earthquake-to-earthquake triggering.

However, in volcanic and geothermal environments, such as the Campi Flegrei caldera, the assumption of a stationary background rate  $\mu$  may be too simplistic. In such systems, transient physical processes (e.g., deformation, magma migration, pore pressure diffusion, thermal stresses) can modulate the crustal stress field, leading to time-dependent variations in the seismicity rate that are not solely caused by earthquake interactions.

### 3.1 Incorporating Non-seismic Forcing via Deformation

We modify the ETAS model by allowing the background rate  $\mu(t)$  to depend explicitly on external aseismic processes, such as deformation. We speculate that  $\mu(t)$  responds to the history of the strain rate  $\dot{\epsilon}(t)$  via a convolution:

$$\mu(t) = \mu_0 \int_0^\infty G(s) \dot{\epsilon}(t - s) ds, \quad (2)$$

where  $\mu_0$  is a scaling factor that converts strain rate into seismicity rate,  $G(s)$  is a causal response kernel encoding the delay and attenuation of the deformation effect and  $s$  is the time lag variable (in days).

To obtain the strain rate from the GNSS displacement time series, we computed a monthly averaged value using a backward 31 day window:

$$\dot{\epsilon}(t) = \frac{D(t) - D(t - \Delta t)}{\Delta t}, \quad (3)$$

where  $D(t)$  is the cumulative deformation measured at time  $t$ , and  $\Delta t = 31$  days. This definition smooths short term fluctuations in the GNSS data and provides a strain-rate time series expressed in units of m/yr. The convolution structure in Eq. (2) reflects the assumption that the crust behaves as a viscoelastic medium, responding to past stress perturbations with characteristic timescales (Hassellmann et al., 1997; Livi et al., 2017; Lucarini, 2018). The kernel  $G(\tau)$  thus acts as a Green's function for the medium, translating external stress inputs into observable seismicity rates.

In our implementation, the kernel  $G(\tau)$  is constructed empirically by correlating cumulative seismic energy release with observed strain. For each shift  $\tau$  in a windowed correlation analysis, we compute:

$$G(\tau) = \frac{\rho(\tau) - \rho_{\min}}{\rho_{\max} - \rho_{\min}}, \quad (4)$$

where  $\rho(\tau)$  is the Pearson correlation coefficient between the strain rate  $\dot{\epsilon}(t)$  and the cumulative seismic energy  $E(t)$  (computed as  $E_i = 10^{1.5m_i}$ , where  $m_i$  is the event magnitude) in a sliding window shifted by  $\tau$  days. Here,  $\rho_{\min} = \min_{\tau} \rho(\tau)$  and  $\rho_{\max} = \max_{\tau} \rho(\tau)$  denote, respectively, the minimum and maximum correlation values obtained over the entire range of time lags considered. The normalization ensures  $G(\tau) \in [0, 1]$ , yielding a unitless empirical kernel. It is important to note that  $G(\tau)$  is estimated here as a single, stationary kernel depending only on the lag  $\tau$ . In principle, one could define a time-varying kernel  $G(\tau, t_j)$  recalculated locally at each reference time  $t_j$ , but in this study we adopt a global kernel to ensure statistical robustness and to maintain a simple formulation directly comparable to the classical ETAS model. This choice provides stable estimates by pooling the entire dataset, while a local kernel would require additional parameters and may suffer from poor constraints due to limited data in each window.

This construction does not assume a specific functional form (e.g., exponential or power-law decay), making it adaptable to the rheological complexity of volcanic environments. The final background rate becomes:

$$\mu(t) = \mu_0 \sum_{i=1}^{N_\tau} G(\tau_i) \dot{\epsilon}(t - \tau_i) \Delta t, \quad (5)$$

where  $\Delta t = 1$  day and  $N_\tau$  is the number of shift values. Here,  $\mu_0$  provides the baseline level of the background rate, while the convolution with  $G(\tau)$  introduces fluctuations around this baseline according to the strain-rate history.

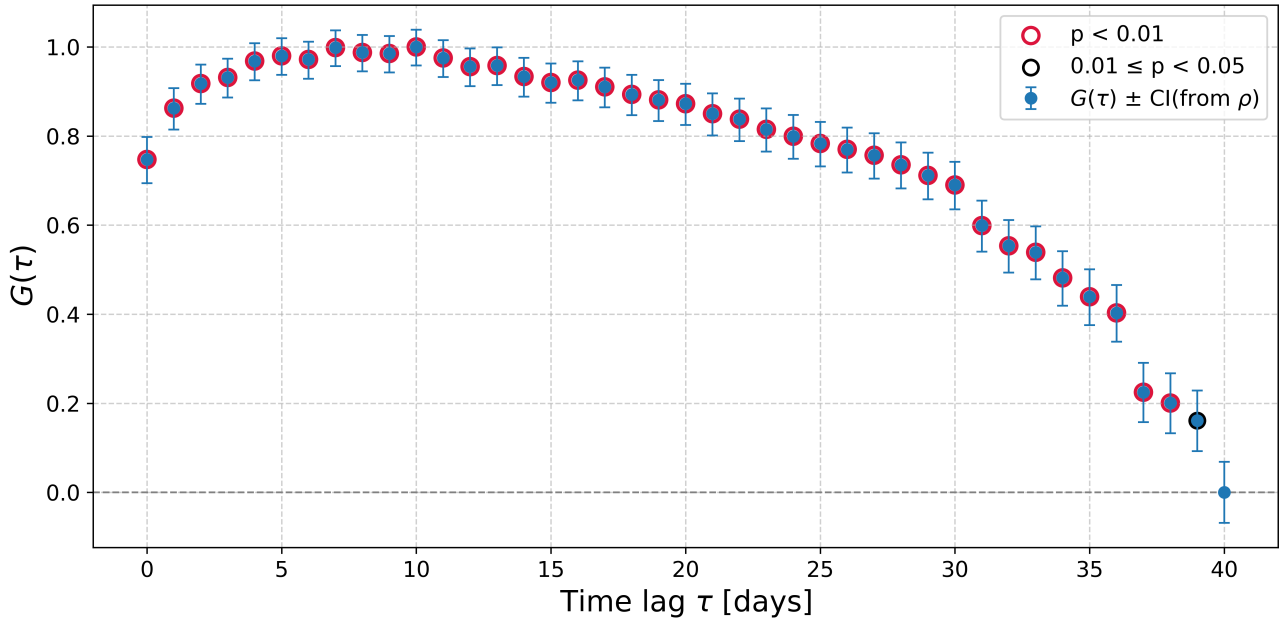
The deformation-driven ETAS model thus defines the conditional intensity as:

$$\begin{aligned} \lambda(t) &= \mu(t) + \sum_{t_i < t} K e^{\alpha(m_i - M_0)} (t - t_i + c)^{-p} \\ &= \mu_0 \sum_{i=1}^{N_\tau} G(\tau_i) \dot{\epsilon}(t - \tau_i) \Delta t \\ &\quad + \sum_{t_i < t} K e^{\alpha(m_i - M_0)} (t - t_i + c)^{-p}, \end{aligned} \quad (6)$$

recovering the classical ETAS model when  $\mu(t) = \mu = \text{const}$ . The novelty of this approach lies in the time dependence of the background term, now informed by an empirical convolution with geodetic data. This allows the model to account for seismicity modulated by aseismic deformation, which is especially relevant in volcanic areas.

### 3.2 Numerical Implementation

We now describe the numerical implementation of the deformation-driven ETAS model in detail. The algorithm consists of the following main steps: (i) reading



**Figure 2** Pearson correlation between strain rate and cumulative seismic energy as a function of time lag  $\tau$ . Blue symbols show  $\rho(\tau)$  with 95% confidence intervals estimated using Fisher r-to-z transformation. Red circles mark correlations significant at  $p < 0.01$ , while black circles indicate  $0.01 \leq p < 0.05$ . The analysis is performed using a 30-day backward window, with the correlation at each lag computed only if more than 10 valid pairs are available. The maximum correlation is observed at lags of about 7 – 12 days, suggesting a delayed response of seismicity to deformation.

and preprocessing of seismic and deformation data; (ii) construction of the empirical response kernel; (iii) computation of the time-dependent background rate  $\mu(t)$ ; (iv) evaluation of the log-likelihood; and (v) optimization of the ETAS parameters.

**(i) Data preprocessing.** We discard the seismic events below a completeness threshold  $M_{th}$  and each magnitude  $m_i$  is converted into seismic energy via the empirical relation

$$E_i = 10^{1.5m_i}, \quad (7)$$

where the additive constant in the original formulation is omitted since only relative variations are required in our analysis. In our catalog, magnitudes are reported in the duration scale  $M_d$ . We note that  $M_d$  was originally calibrated to be consistent with  $M_L$  (Lee et al., 1972), and  $M_L$  is widely accepted as a good proxy for  $M_w$  for small to moderate events ( $M < 4.5$ ), with differences typically below 0.2 units (Hanks and Kanamori, 1979). Therefore, the use of  $M_d$  in Eq. 7 is appropriate as a relative proxy for seismic energy release in our dataset.

**(ii) Empirical kernel estimation.** The response kernel  $G(\tau)$  is computed empirically by correlating strain rate data with cumulative seismic energy. For each time shift  $\tau$  in the range  $[0, 40]$  days, we define a sliding window of fixed length (30 days), and for each window centered at  $t_j$  in the deformation time series, we compute:

1. the cumulative seismic energy released in the window  $[t_j - (30 - \tau), t_j + \tau]$ ;
2. the Pearson correlation  $\rho(\tau)$  between the cumulative energy time series and the strain data;

The final kernel is obtained by normalizing  $\rho(\tau)$  as in Equation 4. This provides a unitless empirical kernel with support on a 41-day discrete lag grid spanning lags from 0 to 40 days, with each correlation computed over a 30 day sliding window of seismic energy.

In practice, we evaluate  $\rho(\tau)$  for lags  $\tau \in [0, 40]$  days, which represents a physically plausible range for the delayed response of volcanic systems, where processes such as pore-pressure diffusion, fluid migration, and viscoelastic stress adjustment typically operate on timescales of days to weeks. Empirically, the correlation decays to negligible values for  $\tau > 40$  days (Figure 2), so extending the lag range further does not provide additional information. A sliding window of 30 days is adopted in order to ensure statistical robustness of the correlation estimates: shorter windows would often contain very few small events ( $M < 4$ ), resulting in unstable values, whereas a 30-day window smooths high-frequency noise while still capturing the month-scale variability of the strain-seismicity coupling.

It is important to note that the adopted backward-sliding scheme implies that for  $\tau = 0$  the cumulative energy is evaluated in the interval  $[t_j - 30, t_j]$ , while for increasing values of  $\tau$  the window progressively shifts forward. For  $\tau \geq 30$ , the window lies entirely after  $t_j$ , e.g.,  $[t_j, t_j + 30]$  for  $\tau = 30$ . This design is adopted in order to capture possible synchronous, delayed, or slightly anticipatory relationships between deformation and seismicity. In volcanic systems, the relative timing between deformation and earthquakes is not strictly causal and can vary depending on the underlying process (e.g., pore-pressure diffusion, fluid migration, or viscoelastic stress adjustment). The 30 day window length provides enough events for a stable correlation estimate, while



the lag parameter  $\tau$  explores the range of possible temporal relationships between the two signals.

**(iii) Time-dependent background rate.** Given the empirical kernel  $G(\tau)$  and the averaged strain rate  $\dot{\epsilon}(t)$ , we define a dimensionless background shape function  $\mu(t)$  by summing the weighted strain contributions over a finite causal window:

$$\mu(t) = \sum_{i=0}^{N_\tau} G(\tau_i) \dot{\epsilon}(t - \tau_i) \Delta t, \quad (8)$$

where  $\tau_i \in \{0, 1, \dots, 40\}$  days are the discrete lags, and  $\Delta t = 1$  day is the discretization step. Note that the case  $\tau = 0$  is included only as a diagnostic to test for an instantaneous coupling; for actual forecasting the formulation is causal and uses only  $\tau \geq 1$ .

This shape function is normalized via min-max rescaling to the interval  $[0.1, 1.1]$ , ensuring numerical stability and positivity:

$$\mu(t) \leftarrow \frac{\mu(t) - \min_t \mu(t)}{\max_t \mu(t) - \min_t \mu(t)} + \delta, \quad \delta = 0.1.$$

The actual background rate used in the ETAS conditional intensity is then defined as:

$$\mu_{\text{eff}}(t) = \mu_0 \cdot \mu(t), \quad (9)$$

where  $\mu_0$  (in units of events/day) is a constant free parameter estimated during the likelihood maximization. It controls the overall amplitude of the background rate, while  $\mu(t)$  provides its time modulation based on the observed deformation history.

To evaluate  $\mu(t)$  at arbitrary event times  $t_i$ , we first compute  $\mu(t)$  at discrete points (corresponding to the catalog event times), and then interpolate these values with a spline function. This provides a continuous representation of  $\mu(t)$ , which is required for the evaluation of  $\lambda(t)$  during the likelihood optimization.

**(iv) Log-likelihood function.** The log-likelihood  $\mathcal{L}(\theta)$  is written as:

$$\mathcal{L}(\theta) = \sum_{i=1}^N \log \lambda(t_i) - \int_{T_1}^{T_N} \lambda(t) dt, \quad (10)$$

with the conditional intensity given by:

$$\lambda(t) = \begin{cases} \mu_0 \mu(t) & \text{(background)} \\ + \sum_{t_j < t} K_0 e^{\alpha(m_j - M_0)} (t - t_j + c)^{-p} & \text{(triggering)} \end{cases} \quad (11)$$

The first term of  $\mathcal{L}$  is computed directly by evaluating  $\lambda(t_i)$  for each observed event.

The second term, the time integral of  $\lambda(t)$  over the observation interval, has two components: the background integral:  $\int_{T_1}^{T_N} \mu_0 \mu(t) dt$  and the triggering integral  $\sum_{j=1}^N \int_{t_j}^{T_N} K_0 e^{\alpha(m_j - M_0)} (t - t_j + c)^{-p} dt$ . The temporal integral is computed analytically:

$$\int_{t_j}^{T_N} \frac{dt}{(t - t_j + c)^p} = \begin{cases} \frac{(T_N - t_j + c)^{1-p} - c^{1-p}}{1-p}, & p \neq 1, \\ \log \left( \frac{T_N - t_j + c}{c} \right), & p = 1, \end{cases} \quad (12)$$

Thus, the total triggering integral is:

$$\sum_{j=1}^N K_0 e^{\alpha(m_j - M_0)} A_j, \quad (13)$$

where  $A_j$  is the analytical expression Eq.(12).

**(v) Optimization and parameter bounds.** We define the parameter vector as  $\theta = (\mu_0, K_0, c, \alpha, p)$ , and perform numerical minimization of  $-\mathcal{L}(\theta)$  via quasi-Newton algorithm. Parameter bounds are imposed to ensure physical plausibility:

$$\mu_0 > 0, \quad K_0 > 0, \quad c \geq 10^{-5}, \quad \alpha \geq 10^{-3}, \quad p \in [0.5, 2.5].$$

Initial guesses are set to:

$$\mu_0 = 0.01, \quad K_0 = 0.02, \quad c = 0.001, \quad \alpha = 1.0, \quad p = 1.1.$$

Convergence is declared when the relative change in the objective function and the gradient norm fall below  $10^{-6}$ . In order to verify the robustness of the maximum likelihood solution, we repeated the optimization using several different sets of initial parameter values. The results were consistent across runs, indicating that the estimated parameters are not sensitive to the choice of initial conditions.

## 4 Results

To quantify the empirical response of seismicity to deformation, we estimate the kernel  $G(\tau)$  via the Pearson correlation between the strain rate  $\dot{\epsilon}(t)$  and the cumulative seismic energy released in the following time window. For each lag  $\tau$ , we compute the correlation between  $\dot{\epsilon}(t)$  and the energy released between  $t + \tau$  and  $t + \tau + 30$  days. The resulting kernel is normalized between 0 and 1 and shown in Figure 2. Before normalization, the correlation coefficient  $\rho(\tau)$  varies in the standard range  $[-1, 1]$ , with values peaking around  $\tau \approx 8 - 12$  days. In our case, the maximum correlation is about 0.6.

The kernel displays a clear peak at approximately  $\tau = 10$  days, suggesting that deformation has the strongest influence on seismicity roughly ten days later. This supports the hypothesis of a delayed triggering mechanism mediated by stress diffusion or fluid migration processes.

Based on the estimated kernel  $G(\tau)$ , we compute a time-dependent background rate  $\mu(t)$  as a convolution of  $\dot{\epsilon}(t)$  with the empirical kernel. This background rate enters the ETAS model as a modulating term that varies with time according to the strain rate history.

We compare two models:

1. A **stationary ETAS model**, where the background rate  $\mu_0$  is constant.
2. A **deformation-driven ETAS model**, where the background rate is  $\mu_{\text{eff}}(t) = \mu_0 \cdot \mu(t)$ , with  $\mu(t)$  computed from strain rate as described above.

The optimal parameters obtained from maximum likelihood estimation are summarized in Table 1.

**Table 1** Estimated ETAS parameters for the stationary and deformation-driven models.

Parameter	Stationary Model	Deformation-Driven Model
$\mu_0$ [events/day]	0.0084	0.026
$K_0$	0.057	0.055
$c$ [days]	$2.8 \times 10^{-4}$	$3.0 \times 10^{-4}$
$\alpha$	0.47	0.48
$p$	0.94	0.95
AIC	638	634

The deformation-driven model achieves a lower AIC compared to the stationary model, indicating a better trade-off between model complexity and goodness of fit. According to the AIC comparison ( $\Delta AIC \simeq 4$ ), the deformation dependent ETAS model provides a better fit than the stationary version, in line with the guidelines of Burnham and Anderson (2002), which consider such differences as providing considerable support for the better model.

Table 1 shows that while the short-term triggering parameters ( $K_0, \alpha, c, p$ ) are broadly consistent between the stationary and deformation driven ETAS models, the background rate differs. In the stationary case,  $\mu_0$  is constant, whereas in the deformation driven model the effective background rate is modulated by the strain rate, leading to a smaller estimated  $\mu_0$ . This redistribution of seismicity between background and triggered components highlights the impact of including deformation in the model.

Figure 3 illustrates the temporal evolution of the background rate  $\mu(t)$  estimated in the deformation driven model. Compared to the stationary estimate ( $\mu_0 = 0.0084$ ), the background rate exhibits strong time variability, reaching values more than two orders of magnitude larger during periods of enhanced strain rate.

We observe that the peaks in  $\mu(t)$  align with periods of elevated strain rate. Conversely, during intervals of low strain rate, the background rate falls. This indicates a positive correlation between deformation and seismic productivity, consistent with the results of the empirical kernel analysis.

## 5 Discussions and Conclusions

We introduced a deformation-driven ETAS model that incorporates geodetic observations into the background rate term of the classical ETAS formulation. The background rate  $\mu(t)$  is no longer assumed to be constant, but instead varies as a convolution of the strain rate  $\dot{\epsilon}(t)$  with an empirically derived response kernel. This approach allows for a flexible, data-driven way to couple aseismic processes to seismicity rates.

The empirical kernel estimated in this study shows a clear peak at a lag of approximately 10 days, indicating that seismic energy release is maximally correlated with strain rate occurring 10 days earlier. We stress that this lag is an empirical feature of the Campi Flegrei dataset, rather than a universal constant. While such a delay could be qualitatively consistent with mecha-

nisms such as viscoelastic relaxation or fluid migration, we emphasize that this interpretation remains a working hypothesis and not direct evidence of a specific physical process.

Comparison with a standard stationary ETAS model demonstrates that incorporating deformation leads to positive evidence of improvement in model performance, as measured by the Akaike Information Criterion (AIC). The difference in AIC supports the hypothesis that time-dependent deformation processes modulate the background seismicity in the Campi Flegrei caldera.

In addition, the temporal evolution of  $\mu(t)$  aligns well with periods of elevated strain rate, further confirming the physical relevance of the coupling.

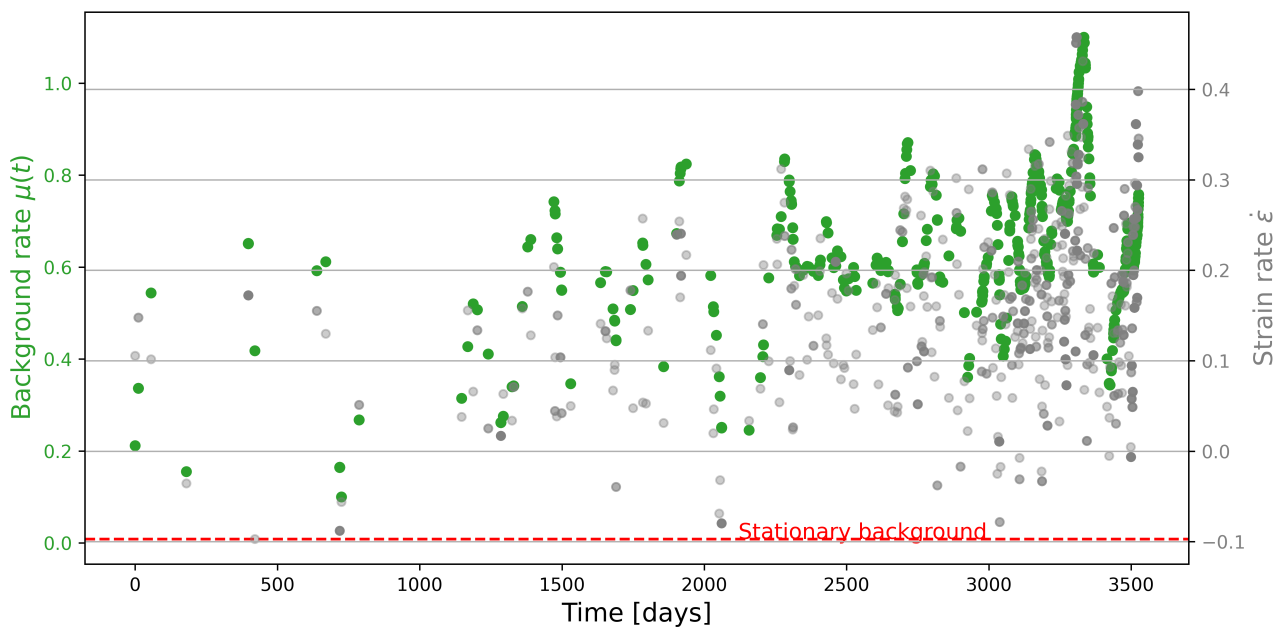
The deformation ETAS model is conceptually simple and can be adapted to any geodetic signal that can be related to strain or stress (e.g., GPS, InSAR, tiltmeters). It does not require prior assumptions about the shape of the kernel, making it suitable for complex, heterogeneous environments such as calderas and geothermal fields.

However, several limitations remain. First, the empirical kernel estimation assumes a linear response and may not fully capture nonlinear or threshold behaviors in the deformation–seismicity coupling. Second, the model relies on high-quality, high-frequency strain data, which may not be available in all regions and in real-time. Third, the normalization of  $\mu(t)$  introduces some arbitrariness in the amplitude of the background rate, although this is partially mitigated by estimating a global scaling factor  $\mu_0$ . Fourth, in this study we relied on the RITE GNSS station to compute the strain rate. This choice is motivated by the fact that Campi Flegrei deformation is largely characterized by a radially symmetric uplift centered beneath Pozzuoli (De Natale et al., 2006), for which RITE provides a representative proxy. Nevertheless, we acknowledge that spatial heterogeneity of seismic clusters may not be fully captured by a single station, and future developments should consider a multi-station or spatially distributed approach to reduce potential biases.

From a physical perspective, the deformation term  $\mu(t)$  can be interpreted as the seismic response of a nonequilibrium crustal system to an external perturbation. Following linear response theory, the system's state (here, the earthquake rate) reacts linearly to weak, time-dependent forcing, with the kernel  $G(\tau)$  reflecting the viscoelastic properties of the medium. A fast-decaying  $G(\tau)$  implies rapid stress dissipation (e.g., brittle behavior), whereas a slowly decaying or broad kernel corresponds to delayed triggering due to fluid diffusion or ductile flow.

This formulation is consistent with studies on fluid-induced seismicity, where the rate of earthquakes follows a convolution between the fluid injection rate and a response kernel (Kim and Avouac, 2023; Shcherbakov, 2024). In our case, the forcing is not injection but natural strain accumulation, and the method generalizes to tectonic or volcanic deformation patterns.

Future work could address these issues by testing alternative kernel estimation techniques (e.g., deconvolu-



**Figure 3** Temporal evolution of the deformation-driven background rate  $\mu(t)$  (green circles), compared with the observed strain rate  $\dot{\epsilon}(t)$  (gray dots). The red dashed line indicates the stationary background rate obtained in the stationary ETAS model.

tion or regularized inversion), exploring spatially varying background rates, or combining multiple geophysical observables. The deformation ETAS framework could also be extended to forecast seismicity in real-time, provided that continuous strain data are available. To move into an Operational Earthquake Forecasting system, a pseudo-prospective test using independent data is needed to ensure the robustness of our findings.

Overall, our results highlight the value of incorporating geodetic information into statistical seismology models and provide a step toward more physically informed earthquake forecasting frameworks in active volcanic systems. Nonetheless, our findings should be considered preliminary. They provide a first empirical indication that GNSS-based strain rates can inform the background rate in ETAS models, but further work is needed to test the robustness of this framework under pseudo-prospective conditions and across different volcanic environments.

## Acknowledgements

GP acknowledges the Earth Observatory of Singapore (EOS), and the Singapore Ministry of Education Tier 3b project “Investigating Volcano and Earthquake Science and Technology (InVEST)”. MT acknowledges the CPS (Centro di Pericolosità Sismica) of INGV. The authors want to thank Prospero De Martino and Giuseppe Falcone for their help in retrieving the dataset used in this work.

## Data and code availability

All data and code necessary to reproduce the results of this study are publicly available at: <https://doi.org/10.5281/zenodo.16667421>. The seismic catalog is from

Ricciolino et al. (2024).

## Competing interests

The authors declare no competing interests.

## References

- Akaike, H. Information theory and an extension of the maximum likelihood principle, proceedings of the 2nd international symposium on information, bn petrow, f. Czaki, *Akademiai Kiado, Budapest*, 1973.
- Bevilacqua, A., Neri, A., De Martino, P., Giudicepietro, F., Macedonio, G., and Ricciolino, P. Accelerating upper crustal deformation and seismicity of Campi Flegrei caldera (Italy), during the 2000–2023 unrest. *Communications Earth & Environment*, 5(1): 742, 2024.
- Chouet, B. A. Long-period volcano seismicity: its source and use in eruption forecasting. *Nature*, 380(6572):309–316, 1996.
- Console, R., Murru, M., and Lombardi, A. M. Refining earthquake clustering models. *Journal of Geophysical Research: Solid Earth*, 108(B10), 2003.
- Convertito, V., Godano, C., Petrillo, G., and Tramelli, A. Insights from b value analysis of Campi Flegrei unrests. *Scientific Reports*, 15(1):14974, 2025.
- De Martino, P., Dolce, M., Brandi, G., Scarpato, G., and Tammaro, U. The ground deformation history of the neapolitan volcanic area (Campi Flegrei caldera, Somma-Vesuvius Volcano, and Ischia island) from 20 years of continuous GPS observations (2000–2019). *Remote Sensing*, 13(14):2725, 2021.
- De Natale, G., Troise, C., Pingue, F., Mastrolorenzo, G., Pappalardo, L., Battaglia, M., Boschi, E., et al. The Campi Flegrei caldera. Unrest mechanisms and hazard. *Special Publication-Geological Society of London*, 269:25–45, 2006.
- Giudicepietro, F., Avino, R., Bellucci Sessa, E., Bevilacqua, A., Bonano, M., Caliro, S., Casu, F., De Cesare, W., De Luca, C., De Martino, P., et al. Burst-like swarms in the Campi Flegrei caldera

- accelerating unrest from 2021 to 2024. *Nature Communications*, 16(1):1548, 2025.
- Glazner, A. F. and McNutt, S. R. Relationship Between Dike Injection and b-Value for Volcanic Earthquake Swarms. *Journal of Geophysical Research: Solid Earth*, 126(12):e2020JB021631, 2021. doi: <https://doi.org/10.1029/2020JB021631>.
- Godano, C., Convertito, V., Tramelli, A., and Petrillo, G. How Ground Deformation Influences Earthquake Occurrence During the Ongoing Unrest at Campi Flegrei (2005-Present). *arXiv preprint arXiv:2503.20129*, 2025.
- Hainzl, S. Self-organization of earthquake swarms. *Journal of Geodynamics*, 35(1):157–172, 2003. doi: [https://doi.org/10.1016/S0264-3707\(02\)00060-1](https://doi.org/10.1016/S0264-3707(02)00060-1).
- Hainzl, S. and Ogata, Y. Detecting fluid signals in seismicity data through statistical earthquake modeling. *Journal of Geophysical Research: Solid Earth*, 110(B5), 2005.
- Hanks, T. C. and Kanamori, H. A moment magnitude scale. *Journal of Geophysical Research: Solid Earth*, 84(B5):2348–2350, 1979. doi: <https://doi.org/10.1029/JB084iB05p02348>.
- Hasselmann, K., Hasselmann, S., Giering, R., Ocan, V., and Storch, H. Sensitivity study of optimal CO2 emission paths using a simplified structural integrated assessment model (SIAM). *Climatic Change*, 37(2):345–386, 1997.
- Herrmann, M. and Marzocchi, W. Inconsistencies and lurking pitfalls in the magnitude–frequency distribution of high-resolution earthquake catalogs. *Seismological Society of America*, 92(2A):909–922, 2021.
- Iervolino, I., Cito, P., De Falco, M., Festa, G., Herrmann, M., Lomax, A., Marzocchi, W., Santo, A., Strumia, C., Massaro, L., et al. Seismic risk mitigation at Campi Flegrei in volcanic unrest. *Nature communications*, 15(1):1–14, 2024.
- Kim, T. and Avouac, J.-P. Stress-based and convolutional forecasting of injection-induced seismicity: Application to the Otaniemi geothermal reservoir stimulation. *Journal of Geophysical Research: Solid Earth*, 128(4):e2022JB024960, 2023.
- Kumazawa, T. and Ogata, Y. Quantitative description of induced seismic activity before and after the 2011 Tohoku-Oki earthquake by nonstationary ETAS models. *Journal of Geophysical Research: Solid Earth*, 118(12):6165–6182, 2013.
- Kumazawa, T. and Ogata, Y. Nonstationary ETAS models for non-standard earthquakes. *The Annals of Applied Statistics*, 8(3): 1825, 2014.
- Lee, W., Bennett, R., and Meagher, K. A method of estimating magnitude of local earthquakes from signal duration. *U.S. Geological Survey Open-File Report*, 72-223:1–28, 1972. doi: [10.3133/ofr72223](https://doi.org/10.3133/ofr72223).
- Livi, R., Politi, P., et al. Nonequilibrium statistical physics: A modern perspective. 2017.
- Lucarini, V. Revising and extending the linear response theory for statistical mechanical systems: Evaluating observables as predictors and predictands. *Journal of Statistical Physics*, 173(6): 1698–1721, 2018.
- Mizrahi, L., Dallo, I., van der Elst, N. J., Christophersen, A., Spasiani, I., Werner, M. J., Iturrieta, P., Bayona, J. A., Iervolino, I., Schneider, M., et al. Developing, testing, and communicating earthquake forecasts: Current practices and future directions. *Reviews of Geophysics*, 62(3):e2023RG000823, 2024.
- Ogata, Y. Statistical Models for Earthquake Occurrences and Residual Analysis for Point Processes. *Research Memo. (Technical report) Inst. Statist. Math., Tokyo.*, 288, 1985.
- Ogata, Y. Statistical Models for Earthquake Occurrences and Residual Analysis for Point Processes. *J. Amer. Statist. Assoc.*, 83:9 – 27, 1988.
- Ogata, Y. Space-time point-process models for earthquake occurrences. *Annals of the Institute of Statistical Mathematics*, 50: 379–402, 1998.
- Petrillo, G. and Lippiello, E. Testing of the foreshock hypothesis within an epidemic like description of seismicity. *Geophysical Journal International*, 225(2):1236–1257, 2021.
- Petrillo, G. and Lippiello, E. Incorporating foreshocks in an epidemic-like description of seismic occurrence in Italy. *Applied Sciences*, 13(8):4891, 2023.
- Petrillo, G. and Zhuang, J. Bayesian earthquake forecasting approach based on the epidemic type aftershock sequence model. *Earth, Planets and Space*, 76(1):78, 2024.
- Petrillo, G., Kumazawa, T., Napolitano, F., Capuano, P., and Zhuang, J. Fluids-triggered swarm sequence supported by a nonstationary epidemic-like description of seismicity. *Seismological Research Letters*, 95(6):3207–3220, 2024.
- Ricciolino, P., Lo Bascio, D., and Esposito, R. GOSSIP-Database sismologico Pubblico INGV-Osservatorio Vesuviano. *Istituto Nazionale di Geofisica e Vulcanologia (INGV)*, 2024.
- Shcherbakov, R. A stochastic model for induced seismicity at the geothermal systems: A case of the geysers. *Seismological Research Letters*, 95(6):3545–3556, 2024.
- Toda, S., Stein, R., and Sagiya, T. Evidence from the AD 2000 Izu islands earthquake swarm that stressing rate governs seismicity. *Nature*, 419:58–61, 2002. doi: <https://doi.org/10.1038/nature00997>.
- Tramelli, A., Godano, C., Ricciolino, P., Giudicepietro, F., Caliro, S., Orazi, M., De Martino, P., and Chiodini, G. Statistics of seismicity to investigate the Campi Flegrei caldera unrest. *Scientific reports*, 11(1):7211, 2021.
- Zhuang, J., Ogata, Y., and Wang, T. Data completeness of the Kumamoto earthquake sequence in the JMA catalog and its influence on the estimation of the ETAS parameters. *Earth, Planets and Space*, 69(1):1–12, 2017.

The article *Adding strain rate information into a short-term seismicity model improves forecasting performances: the case of Campi Flegrei, Italy* © 2025 by Giuseppe Petrillo is licensed under CC BY 4.0.